Med Biol Eng Comput
DOI 10.1007/s11517-013-1131-9

ORIGINAL ARTICLE

Age estimation using cortical surface pattern combining thickness with curvatures

Jieqiong Wang · Wenjing Li · Wen Miao · Dai Dai · Jing Hua · Huiguang He

Received: 22 April 2013 / Accepted: 8 November 2013

Abstract Brain development and healthy aging have been proved to follow a specific pattern, which, in turn, can be applied to help doctors diagnose mental diseases. In this paper, we design a cortical surface pattern (CSP) combining the cortical thickness with curvatures, which constructs an accurate human age estimation model with relevance vector regression. We test our model with two public databases. One is the IXI database (360 healthy subjects aging from 20 to 82 years old were selected), and the other is the INDI database (303 subjects aging from 7 to 22 years old were selected). The results show that our model can achieve as small as 4.57 years deviation in the IXI database and 1.38 years deviation in the INDI database. Furthermore, we employ this surface pattern to age groups classification and get a remarkably high accuracy (97.77 %) and a significantly high sensitivity/specificity (97.30/98.10 %). These results suggest that our designed CSP combining thickness with curvatures is stable and sensitive to brain development, and it is much more powerful than voxel-based morphometry used in previous methods for age estimation.

Keywords Age estimation · Cortical surface pattern · Thickness · Curvatures

1 Introduction

Normal brain development across the life span is affected by progressive and regressive neuronal processes due to cell growth and death [26]. And this brain development has been proved to follow a specific pattern during the normal aging process [10, 16, 17, 20, 30]. In terms of volume measure, study [10] showed a specific pattern of linear decline in gray matter (GM) with a significantly steeper decline in males, linear increase in cerebrospinal fluid as well as relative accelerated loss of white matter (WM) in local areas (frontal white matter, optic radiations, and so on) under normal aging by investigating 465 subjects aging from 17 to 79 years. Besides, evidences were provided [20, 30] for a region-specific and nonlinear pattern of neurodegenerative age-related GM volume changes. Recently, Taki et al. [29] studied 1,460 healthy individuals aged 20–69 years and revealed a significantly negative correlation between gray matter ratio (gray matter volume divided by intracranial volume) and age in both genders. In terms of surface measure, Shaw et al. [25] demonstrated that the complexities of cortical thickness development trajectories are different in different cortical regions by exploring 375 subjects aging from 3.5 to 33 years. Lemaitre et al. [16] revealed a concomitant global age-related reduction in cortical thickness, surface area, and volume by linear regressions of age. Pienaar et al. [18] showed that curvature measures and functions with a gradual decline through early childhood and further decline continuing through to adults. In 2010, the study by Ronan et al. [22] indicated that there was a relationship between differential development

Electronic supplementary material The online version of this article (doi:10.1007/s11517-013-1131-9) contains supplementary material, which is available to authorized users.

J. Wang · W. Li · W. Miao · D. Dai · H. He (✉)
State Key Laboratory of Management and Control for Complex Systems, Institute of Automation, Key Laboratory of Molecular Imaging of Chinese Academy of Sciences, Institute of Automation, Chinese Academy of Sciences, Beijing 100190, China
e-mail: huiguang.he@ia.ac.cn

J. Hua
Department of Computer Science, Wayne State University, Michigan, USA

Published online: 07 January 2014

and mean curvature. Recently, significant cortical thinning of parietal and insula region was observed during healthy aging while surface area and mean curvature were less affected by aging [17]. These studies suggest certain relationship exists between the brain pattern and human age. Hence, there is a probability to estimate human age from the brain pattern.

Furthermore, mental disorders such as schizophrenia or Alzheimer's disease (AD) arise due to deflections from the normal brain pattern [4, 13, 21]. The estimated age with the deflected brain pattern is consequently far away from the true age, namely the gap between estimated age and the true age of the patient is larger than that of the normal people, which can be used to help doctors diagnose diseases. Thus, human age estimation catches more attention recently.

To our best of knowledge, only a few studies focused on age estimation based on structural MRI or resting-state MRI scans [1, 2, 6, 9]. Dosenbach et al. [6] used SVM regression with resting-state functional connectivity to generate a predicted "brain age" as an estimate of each subject's functional maturity level. Brown et al. [2] applied multimodal image features to age estimation and obtained very small mean error and high correlation coefficient. However, the age ranges of subjects used in these two studies are relatively narrow. Ashburner et al. [1] and Franke et al. [9] utilized a relevance vector machine (RVM) with voxel-based features to estimate the ages of subjects with large age range. But this voxel-based method (voxel-based morphometry, VBM) is purely based on a volumetric representation of the brain. The local amount of tissue is simply measured as the intensity within each voxel, and the measure can be affected by local cortical folding as well as local cortical thickness. Moreover, VBM contains no information about brain surface gyri and sulci, which is very important to age estimation [16, 17].

Since surface-based features have been shown to be more sensitive to age-related decline than VBM [12], we build an age estimation model with surface-based features to overcome the aforementioned limitations [32]. The main contribution of our work is that we develop a reliable cortical surface pattern (CSP) combining cortical thickness and surface curvatures to estimate human ages. The CSP is applied to estimate the age of 663 subjects (age range 7–82) from two publicly accessible databases. The estimation results based on the large-scale datasets with the wide age range demonstrates the precision of our age estimation model using CSP. Furthermore, we employ the CSP to age groups classification. The high cross-validation (CV) accuracy and the high sensitivity/specificity constitute a powerful evidence of the reliability of our designed surface pattern for age estimation.

2 Material, pipeline of age estimation model and experiments

2.1 Databases and subjects

We used two publicly available databases to test our age estimation model in this study. One was the Information extraction from Images (IXI) database (http://www.brain-development.org/) and the other was the International Data-sharing Initiative (INDI) database (ADHD-200 Global Competition, http://fcon_1000.projects.nitrc.org/indi/adhd200/index.html). Several subjects were excluded according to the following schemes: (1) the subjects without age information were excluded; (2) we only retain subjects with the good-quality images; (3) we excluded subjects whose images failed in the feature extraction. A total of 360 normal subjects aged 20–82 years (age $\pm$ SD $=$ 47.04 $\pm$ 16.16, male/female: 175/185) were selected from IXI database, and 303 normal subjects aged 7–22 years (age $\pm$ SD $=$ 11.80 $\pm$ 2.90, male/female: 162/141) were chosen from the INDI database. Table 1 gives the characteristics of the subjects from these two databases. And the MRI scanning parameters are described in the supplementary.

2.2 Pipeline of age estimation model

Figure 1 gives the pipeline of our age estimation model. In the model, we employed two kinds of surface-based features (individual regional features and combined regional features) in relevance vector regression (RVR), respectively. We applied linear search to choose the kernel width of RVR and cross validation (CV) to evaluate the goodness of the kernel width (inner CV). Then, in order to evaluate the model, 10-fold CV (outer CV) was operated 10 times to compute mean absolute error (MAE), root mean squared error (RMSE), and correlation coefficient (corr). Details will be introduced in the following section.

2.2.1 Surface-based features extraction

Structure images were processed by the software FreeSurfer version 5.0.0 (http://surfer.nmr.mgh.harvard.edu/). FreeSurfer is a set of tool for the analysis and visualization of structural and functional brain imaging data. In the

Table 1 The information of different databases used in age estimation model stability analysis

	IXI database	INDI database
Num (M/F)	360 (175/185)	303 (162/141)
Age mean $\pm$ SD	47.04 $\pm$ 16.16	11.80 $\pm$ 2.90
Age range	20–82	7–22

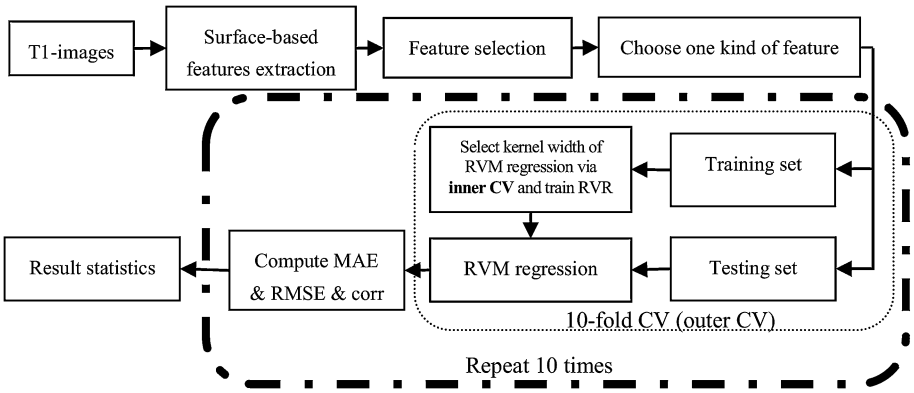

Fig. 1 The pipeline of age estimation model

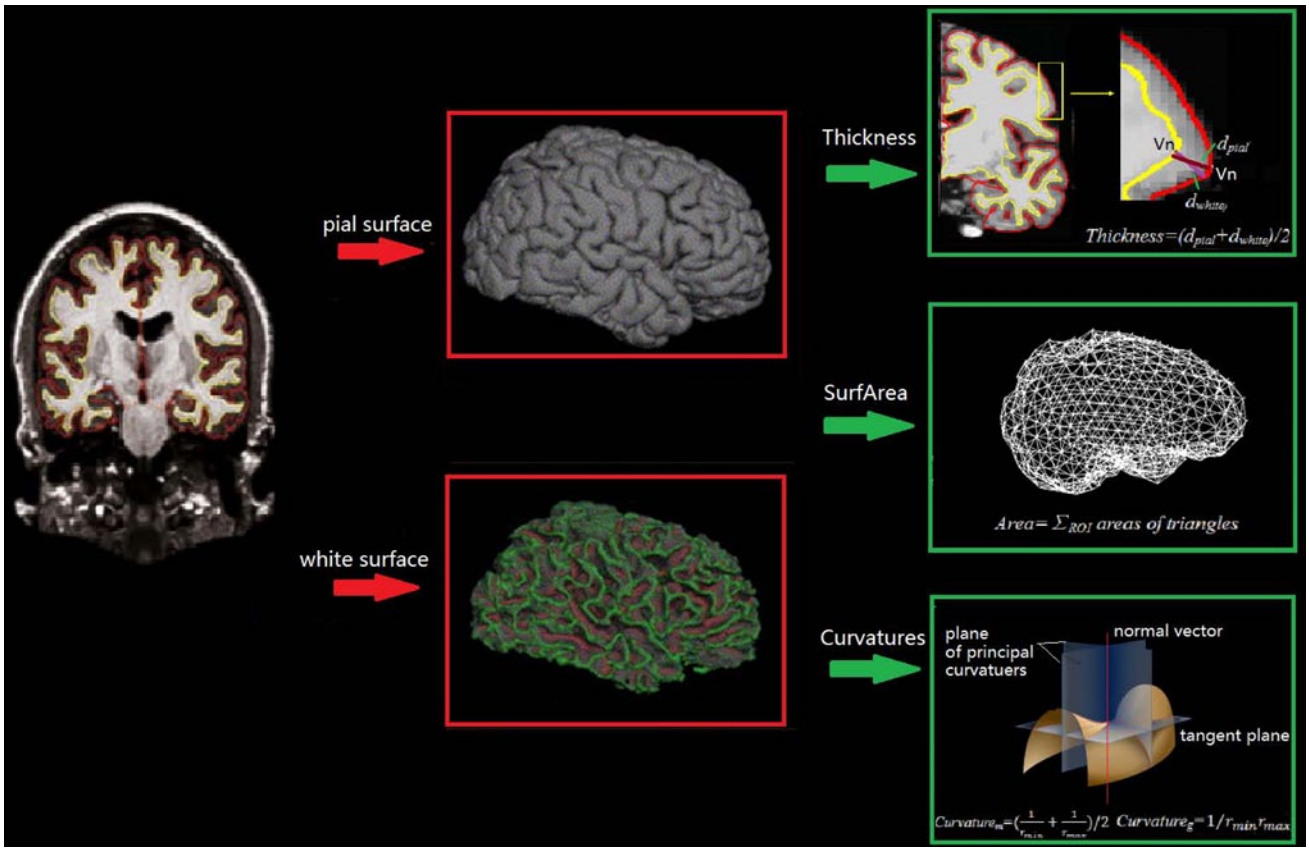

Fig. 2 Surface-based feature extraction by FreeSurfer version 5.0.0

work, we used FreeSurfer to reconstruct cortical surfaces and calculated surface-based features. The details are as follows (Fig. 2).

Preprocess All subjects' T1-weighted images were firstly nonuniform intensity corrected. After image corrections, we scaled the intensities for all voxels. Then, the scaled images were skull-stripped [23]. Subsequently, voxels were classified as the white matter/nonwhite matter. A mesh of triangular faces was then tightly around this mass. The mesh was smoothed, inflated, and corrected topological defects [8, 24] to construct a surface. This surface was used as the starting point for a deformable algorithm to produce the white surface (GM/WM interface) and the pial surface [3]. Then, we calculated cortical thickness, surface area, and curvatures based on the pial/white surface.

Cortical thickness The measurement of cortical thickness was explained in the paper [7]. In brief, cortical thickness was defined as the distance between linked vertexes on the white and pial surfaces. The correspondence between such vertexes was created by the expansion of the pial

Table 2 All features used in age estimation

Individual regional features	Combined regional features
Thickness (thick)	Thickness ∪ surface area (Thick ∪ SurfArea)
Surface area (SurfArea)	Thickness ∪ 2 curvatures (Thick ∪ 2Curv)
Mean curvature (mCurv)	Thickness ∪ surface area ∪ 2 curvatures– (Thick ∪ SurfArea ∪ 2Curv)
Gaussian curvature (gCurv)	

surface from the white surface. The distance between the vertex of white surface and the linked vertex of pial surface was defined as the thickness at each location of vertex (Fig. 2).

Surface area We smoothed the white surface before surface area calculation. The smoothed white surface was represented as triangle-based mesh in FreeSurfer. Subsequently, the surface area was defined as the sum of areas of triangles in the region of interest (ROI) on the smoothed white surface (Fig. 2).

Curvatures The smoothed white surface was inflated to produce the inflated surface. Then, we calculated the unit normal vector at each vertex v of the inflated surface. A normal plane at vertex v was one that contained the normal and would therefore also contain a unique direction tangent to the inflated surface and cut the surface in a plane curve. This curve would in general have different curvatures for different normal planes at vertex v. The principal curvatures at v, denoted k_1 and k_2, were the maximum and minimum values of this curvature (Fig. 2). The two most widely used indexes, mean curvature and Gaussian curvature, were then defined as

$$\text{Mean curvature}: M = \frac{1}{2}(k_1 + k_2) \tag{1}$$

$$\text{Gaussian curvature}: G = k_1 \times k_2 \tag{2}$$

2.2.2 Feature selection

We used region-based features instead of vertex-based features for the following reasons. Firstly, region-based features reduce the noise effects by averaging overall voxels in the region. Secondly, using region-based features can control for Type I error by limiting the number of statistical tests to a few ROIs. Thirdly, performing an ROI analysis is more efficient than vertex-based analysis, since the dimension of features used in vertex-based analysis is too high [19].

The cortical surface was divided into 148 distinct cortical ROIs by Destrieux atlas [5]. After ROIs division, average thickness, average mean curvature, average Gaussian curvature, and surface area of each ROI were all calculated. Therefore, four kinds of individual regional features were obtained. Subsequently, different kinds of individual regional features containing complementary information about age were combined to obtain a pattern for age estimation. Previous studies [16, 17] have found significant cortical thickness thinning in the life span (subjects aged from 18 to 87 years in [16], from 18 to 94 in [17]). Therefore, we inferred that it is essential to include cortical thickness in the combined regional features. We constructed combined features on the basis of cortical thickness as well as surface area, curvatures or both surface area and curvatures, respectively. Then, three kinds of combined regional features were obtained. Note that we denoted the feature of cortical thickness, surface area, and two curvatures as Thick, SurfArea, and 2Curv, respectively. Here, Thick and SurfArea were both 148-dimensional vector, and 2Curv was a vector with 296 dimension. The combination of feature $A = [A_1, A_2, \ldots, A_m]^T$ and feature $B = [B_1, B_2, \ldots, B_n]^T$ was defined as

$$A \cup B = [A_1, A_2, \ldots, A_m, B_1, B_2, \ldots, B_n]^T \tag{3}$$

Both individual features and combined features used in age estimation are shown in Table 2. In addition, SVM-RFE (support vector machine recursive feature elimination) was also employed to further select surface-based features for age estimation [11], and the details are given in the supplementary.

2.2.3 Relevance vector regression (RVR)

Relevance vector machine was proposed by Tipping [31] based on Bayesian estimation for regression (and classification) problem. The sparsity of RVM is induced by the hyperpriors on model parameters in a Bayesian framework with the maximum a posteriori (MAP) principle. L_1-norm-like regularization used in RVM encourages the sum of absolute values to be small, which often drives many parameters to zero and provides significantly fewer basis functions. This property is often important for good generalization [33]. When RVM is used for regression problem, it is noted as RVR.

In our research, we used RVR model to find out the relationship between input *p-dimension* surface-based feature vector $s_l = \left[s_{l1}, s_{l2}, \ldots, s_{lp}\right]^T$ of a subject l and the corresponding target value age_l:

$$\text{age}_l = y(s_l) + \varepsilon_l, \tag{4}$$

where ε_l was the measure noise, assumed as independent and to be mean-zero Gaussian with variance σ^2, i.e.,

$\varepsilon_l \sim N(0, \sigma^2)$. $y(s_l)$ was the real value predictor and defined as a linear combination of kernel functions $K(s_l, s_i)$:

$$y(s_l) = \sum_{i=1}^{N} w_i K(s_l, s_i) + w_0 = \phi(s_l) W, \tag{5}$$

where N was the number of training samples. s_i ($i = 1, 2, \ldots, N$) was the *p-dimension* surface-based features of the ith training sample. $\phi(s_l) = [1, K(s_l, s_1), K(s_l, s_2), \ldots, K(s_l, s_N)]$ was the kernel vector. $W = (w_0, w_1, w_2, \ldots, w_N)^T$ was the adjustable weight vector.

Then,

$$\varepsilon_l = \text{age}_l - y(s_l) = \text{age}_l - \phi(s_l) W \tag{6}$$

Following the assumption of Gaussian noise ($\varepsilon_l \sim N(0, \sigma^2)$), we got

$$p(\text{age}_l | W, \sigma^2) = \left(2\pi\sigma^2\right)^{-1/2} \exp\left[-\frac{1}{2\sigma^2}\left(\text{age}_l - \phi(s_l) W\right)^2\right] \tag{7}$$

Assuming statistical independence of the N training samples, the maximum likelihood estimate for W was given by

$$p(\text{age} | W, \sigma^2) = \left(2\pi\sigma^2\right)^{-N/2} \exp\left[-\frac{1}{2\sigma^2} \| \text{age} - \Phi W \|^2\right] \tag{8}$$

where $\text{Age} = \left[\text{age}_1, \text{age}_2, \ldots, \text{age}_N\right]^T$ was the age values of N training samples and $\Phi = [\phi(s_1), \phi(s_2), \ldots, \phi(s_N)]^T$.

To summarize, the main idea of the RVR was to estimate the weights of the Eq. (5) by maximizing the likelihood function (Eq. 8) and then use the real value predictor $y(s_l)$ to estimate the age of the subject.

2.2.4 Cross validation

We applied linear search to choose the Gaussian kernel width of RVR and an inner CV to evaluate the properness of the kernel width. In order to avoid overfitting and obtain an unbiased results of the age estimation model, ten times tenfold CV [14] (outer CV) was used to evaluate the performance of the model. In each of the tenfold CV, all the subjects were randomly partitioned into 10 equal size subsamples. Of the 10 subsamples, a single subsample was retained as the validation data for testing the model and the remaining 9 subsamples were used as training data. The results were then averaged to produce a single evaluation.

We applied the CV framework to the age estimation model (the predicted age: p_i, the real age: r_i). Then, the accuracy of age estimation accuracy was measured by the mean absolute error and the root mean squared error:

$$\text{MAE} = \frac{1}{N} \sum_{i=1}^{N} |p_i - r_i| \tag{9}$$

$$\text{RMSE} = \left[\frac{1}{N} \sum_{i=1}^{N} (p_i - r_i)^2\right]^{1/2} \tag{10}$$

Besides MAE and RMSE, the correlation coefficient (corr) between predicted age and real age was calculated:

$$\text{corr} = \frac{\sum_{i=1}^{N} (p_i - \bar{p})(r_i - \bar{r})}{\sqrt{\sum_{i=1}^{N} (p_i - \bar{p})^2} \sqrt{\sum_{i=1}^{N} (r_i - \bar{r})^2}} \tag{11}$$

where $\bar{p}$ was the mean value of all the predicted age and $\bar{r}$ was the mean value of all the real age.

2.3 Experiments

2.3.1 Feature analysis

Age estimation models with different surface-based features (Table 2) were applied to 360 subjects from the IXI database, respectively. Data-driven approach was utilized to find the best feature pattern, with which we can obtain the smallest MAE and RMSE and the highest corr of age estimation model. This best feature pattern is defined as the CSP. Consequently, "Choose one kind of feature" in the pipeline of age estimation model (Fig. 1) can be definitely replaced by "Choose the CSP". Furthermore, we used SVM-RFE to check out whether the CSP can be further pruned or not.

In order to reveal why the age estimation model with the CSP performs best, we first calculated the correlation coefficients ($p < 0.05$) between surface-based features and age, and then ranked regional features in terms of correlation coefficients. After that, we investigated the first ten feature (mean value) trajectories across age groups as well as the age effect on the most correlated features.

2.3.2 Reliability of age estimation model using the CSP

Since normal subjects in the IXI database are all adults, to further test our model's reliability to age ranges and databases, we applied the age estimation model using the CSP to the selected 303 normal juveniles from the INDI database. Detailed characteristics of subjects are shown in Table 1.

2.3.3 Age group classification using the CSP

For the purpose of evaluating the efficiency of the CSP, we used the CSP to construct an age group classification for the selected 360 normal subjects (Column 1 of Table 1). For simplicity, here we only classify the young group (aging below 30) and the old group (aging above 60). After selection, there are 74 subjects in the young group and 105

subjects in the old group, respectively. In this classification model, the feature is the CSP and the classifier is multi-kernel learning (MKL, details are in the supplementary) [27]. Here, tenfold CV is utilized to evaluate the performance of the classification model.

Prediction accuracy, sensitivity (true positive rate), specificity (true negative rate), and J-statistic [34] were used to evaluate the classification performance. J-statistic combined measure of sensitivity and specificity and is calculated as sensitivity + specificity—1. The larger J-statistic is, the better the classification performed.

3 Results

3.1 Feature analysis

The prediction results of age estimation model with individual regional surface-based features (Column 1 in Table 2) is shown in Table 3, and it indicates that regional thickness works best among the four kinds of regional features. The prediction results of the model with combined regional surface-based features (Column 2 in Table 2) are shown in Table 4, which demonstrates the combined feature with cortical thickness and cortical curvatures performs best among the combined regional features.

Comparing Table 3 with Table 4, it is clear that using the combined features with two curvatures and thickness gives us the best result (MAE = 4.6 years, RMSE = 5.6 years, corr = 0.94). This result is visualized in Fig. 3. The prediction result of each individual is represented as a point in the figure. The blue line shows the ideal case where predicted age matches real age. All points are very close to the blue line, which demonstrates that the predicted age and the real age are highly correlated (corr = 0.94) and consequently substantiate the age estimation model with thickness and curvatures. Therefore, the CSP we defined before is equivalent to the combined features with cortical thickness and surface curvatures.

In order to investigate whether the CSP could be reduced dimension without losing age information or not, we firstly used SVM-RFE to reduce the dimension of CSP

Table 3 Performance of different individual regional features with RVR based on tenfold cross validation

	Thick	mCurv	gCurv	SurfArea
MAE	**6.05 ± 0.05**	7.88 ± 0.07	11.21 ± .0.10	10.52 ± 0.22
RMSE	**7.37 ± 0.03**	9.55 ± 0.09	13.64 ± 0.15	12.96 ± 0.14
corr	**0.89 ± 0.01**	0.81 ± 0.01	0.55 ± 0.01	0.60 ± 0.01

The bold represents the best performance

Thick regional thickness, *mCurv* regional mean curvature, *gCurv* regional Gaussian curvature, *surfArea* regional surface area

Table 4 Performance of different combined regional features with RVR based on tenfold cross validation

	Thick ∪ surfArea	Thick ∪ 2Curv	Thick ∪ surfArea ∪ 2Curv
MAE	5.97 ± 0.11	**4.57 ± 0.04**	5.06 ± 0.09
RMSE	7.35 ± 0.12	**5.57 ± 0.04**	6.10 ± 0.11
corr	0.89 ± 0.01	**0.94 ± 0.01**	0.93 ± 0.01

The bold represents the best performance

A∪B means the combined feature of feature A and feature B, 2Curv: regional mean curvature regional Gaussian curvature

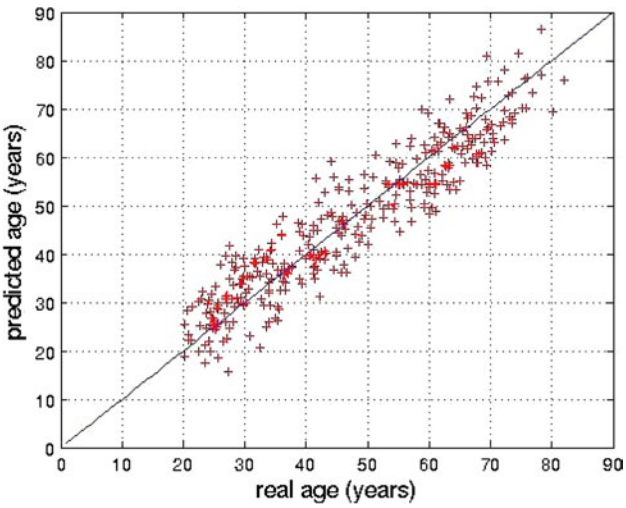

Fig. 3 Visualization of results from the age estimation model. Each point in the figure represents an individual. Both values are highly correlated (corr = 0.94). The *blue line* shows the value where predicted age matches real age (color figure online)

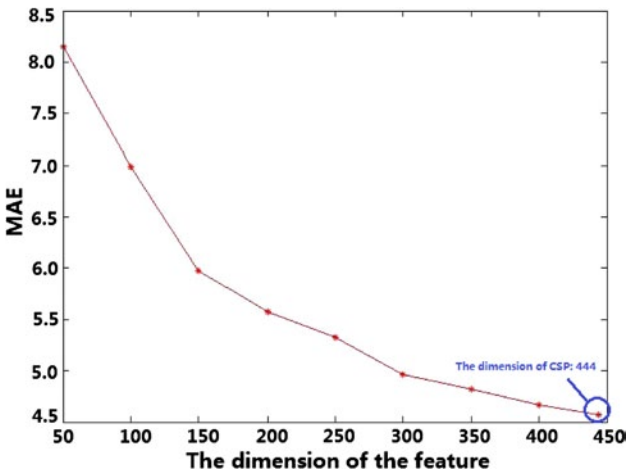

Fig. 4 The trends of MAEs along with different dimensions of selected features (chosen from the CSP by SVM-RFE). The horizontal axis represents the number of the feature combination. The vertical axis represents the MAE of the age estimation model

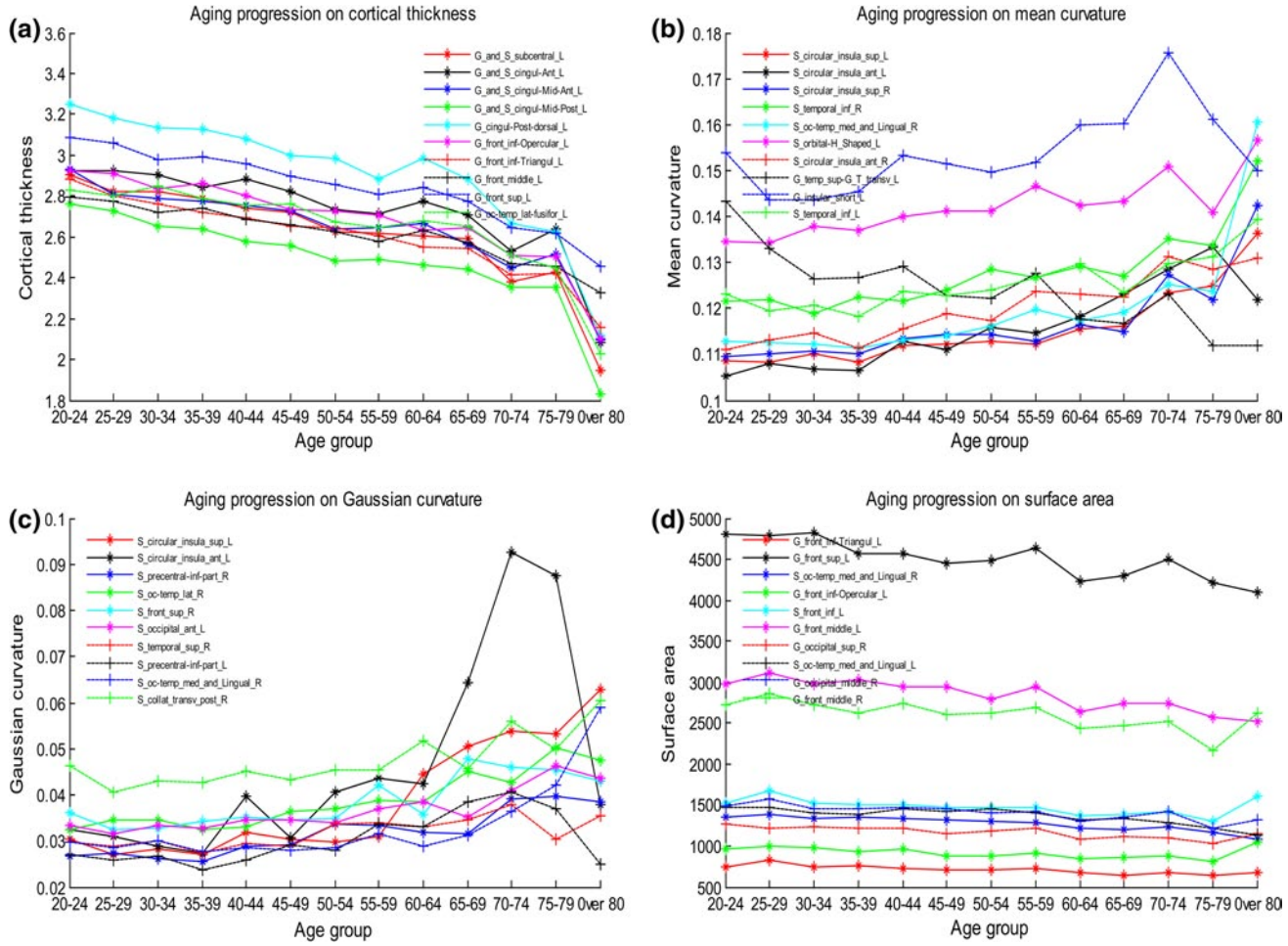

Fig. 5 Age groups effect on four kinds of regional features. The order of regions in the legend is according to the order of correlation coefficients between the region features and age. *G* Gyrus; *S* Sulcus; *L* Left brain. **a** Age groups effect on the first ten most correlated regional cortical thicknesses. **b** Age groups effect on the first ten most correlated regional mean curvatures. **c** Age groups effect on the first ten most correlated regional Gaussian curvatures. **d** Age groups effect on the first ten most correlated regional surface area

to a specified dimension. Then, we applied these selected features in age estimation and calculated the corresponding MAE. The trends of MAEs along with the dimension of features are shown in Fig. 4. The MAE of age estimation decreases as the dimension of the chosen feature increases. This monotone decreasing pattern illustrated in Fig. 4 indicates the CSP obtained by the statistical method has the smallest dimension and cannot be reduced without losing the age information.

The mean values of the first ten features are plotted against age groups for sectional analysis, respectively, in Fig. 5, and the model with the best-fitting robustness was chosen to display the data in Fig. 6. Figure 5 shows that there are different tendencies of thickness and curvatures as well as no changes of surface area across life span in healthy aging. Figure 6 shows that the correlated coefficient of surface area is the smallest among these four kinds of features. Almost no change to surface area across life span and the lowest correlation with human age among all surface-base features suggests the surface area does not have much information about age.

Our estimation model is compared with previous studies [1, 9] using voxel-based features in Table 5. We can clearly see that our model improves about 8 % on MAE and 15 % on RMSE.

3.2 Reliability of age estimation model using the CSP

The performance of age estimation model using the CSP to different databases is given in Table 6 which shows the estimation result of the INDI database is quite well (MAE $= 1.38 \pm 0.02$, RMSE $= 1.77 \pm 0.02$, corr $= 0.79 \pm 0.01$). The age range of subjects in the INDI database is different from that in the IXI database. Overall,

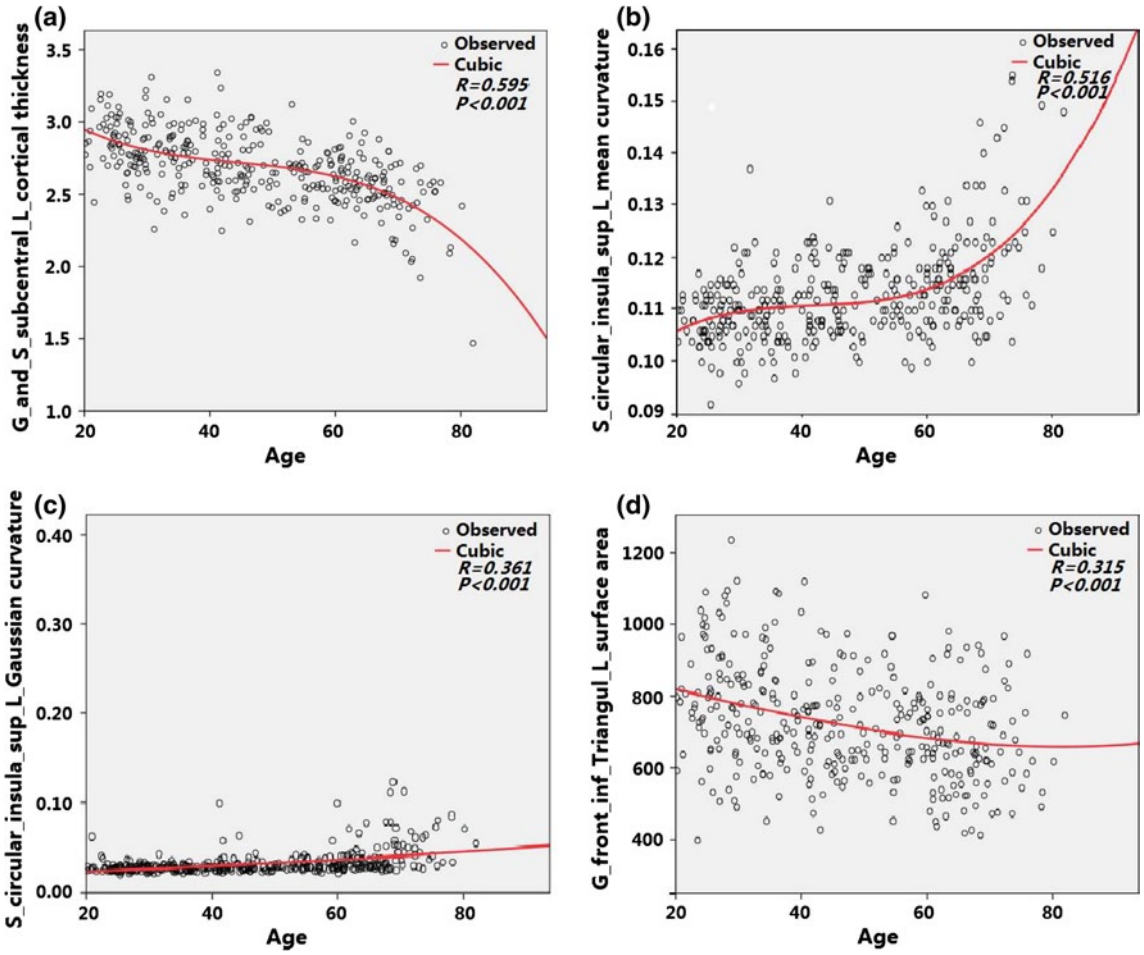

Fig. 6 The best-fitting model between the most correlated features and age. **a** The cubic model ($R = 0.595$, $p < 0.001$) for G_and_S_subcentral_L cortical thickness and age. **b** The cubic model ($R = 0.516$, $p < 0.001$) for S_circular_insula_sup_L mean curvature and age. **c** The cubic model ($R = 0.361$, $p < 0.001$) for S_circular_insula_sup_L Gaussian curvature and age. **d** The cubic model ($R = 0.315$, $p < 0.001$) for G_front_inf_Triangul_L surface area and age

Table 5 Comparing our model with state-of-the-art methods

	Ashburner [1]	Franke [9]	Our model
MAE	—	4.98	**4.57**
RMSE	6.5	6.73	**5.57**
corr	0.86	0.94	0.94

The bold represents the best performance

The notation "---" represents the method doesn't give the corresponding value

Table 6 Performance of age estimation model using the CSP to different databases with RVR based on 10-fold cross validation

(years: Mean ± SD)	IXI database	INDI database
Age range	20–82	2–22
MAE	4.57 ± 0.04	1.38 ± 0.02
RMSE	5.57 ± 0.04	1.77 ± 0.02
corr	0.94 ± 0.01	0.79 ± 0.01

our age estimation model is stable to age ranges as well as databases.

3.3 Age group classification using the CSP

We evaluate the CSP used in our age estimation model by applying it to classify the young group and the old group. Gaussian kernel and different sub-kernel weights are used in MKL for different kinds of features in the pattern, respectively. After tenfold cross validation, we get the classification result of accuracy with 97.77 %, sensitivity with 97.30 %, specificity with 98.10 % and J-statistic with 0.9540. The high CV accuracy (97.77 %) gives the prerequisite of the application of surface pattern while the high sensitivity (97.30 %) and specificity (98.10 %) suggest the classification is little affected by class prior and misclassification cost which is supported by high J-statistic (0.9540) as well. The excellent performance of the classification

further proves that the CSP includes enough age information and can be used for accurate age estimation.

4 Discussion

In the present study, we developed a reliable CSP combining cortical thickness with surface curvatures which is chosen from different kinds of surface-based features, and the MAE/RMSE of age estimation with the CSP is smaller than the previous work whose subjects have wide age range [1, 9].

Comparing with the recent work based on VBM [9], the estimation result improves about 8 % on MAE and 15 % on RMSE (Table 5) on account of employed features and features selection method used in our model. In terms of employed feature, surface-based features were found to be more sensitive to human age than voxel-based features [12, 16, 17]. In terms of feature selection method, we also tried to use PCA to reduce the vertex-based features of the model, but the MAE and RMSE of age estimation were both much larger than that obtained by the model using statistical method. Furthermore, we tried to use SVM-RFE to reduce the dimension of the CSP and we find that the CSP has the smallest dimension and cannot be reduced without losing the age information (Fig. 4). This result suggests that the feature selection in our model is very useful. Therefore, we infer that the improvement is mainly because of the induced surface-based features and the feature selection method used in our model.

In order to reveal why the age estimation model with the CSP performs best, we analyzed the trajectories of surface-based features across life span (Fig. 5) and investigated the age effect on the most correlated features by regression method (Fig. 6). Almost no change to surface area across life span and the lowest correlation with human age among all surface-base features were showed in Figs. 5, 6, suggesting the surface area is not sensitive to human age. This result is consistent with the previous studies [16, 17]. And that's the reason why surface area is not included in surface pattern. The significant tendencies and relatively high correlation between human age and cortical thickness as well as curvatures demonstrate that cortical thickness and curvatures are very sensitive to human age. According to the previous study [18], Gaussian curvature is the intrinsic curvature which concerns the differential relationship between different points on the surface, and mean curvature is the extrinsic curvature which quantifies the rate of deviation between one surface and another. In other words, these two curvatures complement each the other. Although the increased tendency of Gaussian curvature along age groups is not as obvious as that of mean curvature, these two curvatures concern the surface information from different perspectives. We hence both include the two curvatures in the CSP. Moreover, the evident decreased tendency of cortical thickness along age groups indicated that the cortical thickness is quite sensitive to human age, which also coincides with previous researches [16, 17]. Cortical thickness reflects the longitudinal change of cortical cortex along age groups, while two curvatures reflect the transverse change of cortical cortex along age groups. Hence, the CSP reflects cortical changes in both longitudinal direction and transverse direction, which makes CSP perform quite well in the age estimation.

We also utilize the CSP to classify age groups, which gives us a more accurate result than previous studies. Lao et al. [15] tested an SVM-based classification with brain morphometry signature method by assigning their elderly subjects into one of four age groups and reached an accuracy rate of 90 %. Dosenbach et al. [6] performed a binary SVM classification of individual as either children or adults to assess the relative functional brain maturity and reached the accuracy of 91 %. A new MVPA approach based on sparse representation has been employed to investigate the anatomical covariance patterns of normal aging by classifying two age groups in [28] and the mean accuracy is about 97.4 %. Comparing with previous studies, the age groups classification with our CSP yields a high CV accuracy (97.77 %) and a high sensitivity/specificity (97.30/98.10 %). This result indicates that our CSP is sensitive to brain development.

In the recent work, Brown et al. [2] estimated human age with multimodal images and the estimation result was quite well. However, it is difficult to acquire multimodal images because of the high costs on time and money during scanning in the clinical practice. Since we only employ the single-modal images to estimate human age and obtain the high accuracy estimation, our age estimation model using the CSP is of greater practical value. What is more important, our work studied human brain development in almost the whole life span (7–82 years) and demonstrated that a combination of noninvasive brain biomarkers can assess the dynamically changing phases of brain development from early childhood into old adulthood relatively accurately.

In addition, when analyzing the relationship between the surface-based features and human age, we find that, in terms of the regional age-related changes in cortical thickness, predominant reductions were seen in subcentral gyri/sulci, cingulate gyri/sulci, and frontal lobe. In terms of the regional age-related changes in surface area, some regions in the frontal lobe and occipital lobe showed the greatest age-related reduction (Fig. 5). These findings support the previous work [16] and also offer the evidence to prove that cortical thickness is more informative for age-related morphometric changes across the life span, whereas surface area may be less sensitive to morphometric variations with aging than other surface-based features.

5 Conclusions

This paper has presented an age estimation model, which uses the CSP integrating cortical thickness and surface curvatures as features and RVR as the regressor. The experimental results show that our age estimation model improves the prediction accuracy about 8 % on MAE and 15 % on RMSE compared to the previous methods. It suggests that surface-based features are more sensitive to human age than voxel-based features. We also demonstrate that our age estimation model is reliable to age ranges and databases, and the CSP used in the model is sensitive to human age.

Acknowledgments This work was supported in part by 863 Project (2013AA013803), National Natural Science Foundation of China (61271151, 61228103), National Sanitation Foundation (IIS-0915933, IIS-0937586 and IIS-0713315) and National Institutes of Health (1R01NS058802-01, 2R01NS041922-05).

References

1. Ashburner J (2007) A fast diffeomorphic image registration algorithm. Neuroimage 38(1):95–113
2. Brown TT, Kuperman JM, Chung Y, Erhart M, McCabe C, Hagler DJ Jr, Venkatraman VK, Akshoomoff N, Amaral DG, Bloss CS, Casey BJ, Chang L, Ernst TM, Frazier JA, Gruen JR, Kaufmann WE, Kenet T, Kennedy DN, Murray SS, Sowell ER, Jernigan TL, Dale AM (2012) Neuroanatomical assessment of biological maturity. Curr Biol 22(18):1693–1698
3. Dale AM, Fischl B, Sereno MI (1999) Cortical surface-based analysis. I. Segmentation and surface reconstruction. Neuroimage 9(2):179–194
4. Davatzikos C, Xu F, An Y, Fan Y, Resnick SM (2009) Longitudinal progression of Alzheimer's-like patterns of atrophy in normal older adults: the SPARE-AD index. Brain 132(Pt 8):2026–2035
5. Destrieux C, Fischl B, Dale A, Halgren E (2010) Automatic parcellation of human cortical gyri and sulci using standard anatomical nomenclature. Neuroimage 53(1):1–15
6. Dosenbach NUF, Nardos B, Cohen AL, Fair DA, Power JD, Church JA, Nelson SM, Wig GS, Vogel AC, Lessov-Schlaggar CN, Barnes KA, Dubis JW, Feczko E, Coalson RS, Pruett JR, Barch DM, Petersen SE, Schlaggar BL (2010) Prediction of individual brain maturity using fMRI. Science 329(5997):1358–1361
7. Fischl B, Dale AM (2000) Measuring the thickness of the human cerebral cortex from magnetic resonance images. Proc Natl Acad Sci USA 97(20):11050–11055
8. Fischl B, Liu A, Dale AM (2001) Automated manifold surgery: constructing geometrically accurate and topologically correct models of the human cerebral cortex. IEEE Trans Med Imaging 20(1):70–80
9. Franke K, Ziegler G, Kloppel S, Gaser C (2010) Estimating the age of healthy subjects from T1-weighted MRI scans using kernel methods: exploring the influence of various parameters. Neuroimage 50(3):883–892
10. Good CD, Johnsrude IS, Ashburner J, Henson RN, Friston KJ, Frackowiak RS (2001) A voxel-based morphometric study of ageing in 465 normal adult human brains. Neuroimage 14(1):21–36
11. Guyon I, Weston J, Barnhill S, Vapnik V (2002) Gene selection for cancer classification using support vector machines. Mach Learn 46(1–3):389–422
12. Hutton C, Draganski B, Ashburner J, Weiskopf N (2009) A comparison between voxel-based cortical thickness and voxel-based morphometry in normal aging. Neuroimage 48(2):371–380
13. Kirkpatrick B, Messias E, Harvey PD, Fernandez-Egea E, Bowie CR (2008) Is schizophrenia a syndrome of accelerated aging? Schizophr Bull 34(6):1024–1032
14. Kohavi R (1995) A study of cross-validation and bootstrap for accuracy estimation and model selection. In: IJCAI'95 proceedings of the 14th international joint conference on artificial intelligence, vol 2. Morgan Kaufmann Publishers Inc., San Francisco, pp 1137–1145
15. Lao ZQ, Shen DG, Xue Z, Karacali B, Resnick SM, Davatzikos C (2004) Morphological classification of brains via high-dimensional shape transformations and machine learning methods. Neuroimage 21(1):46–57
16. Lemaitre H, Goldman AL, Sambataro F, Verchinski BA, Meyer-Lindenberg A, Weinberger DR, Mattay VS (2012) Normal age-related brain morphometric changes: nonuniformity across cortical thickness, surface area and gray matter volume? Neurobiol Aging 33(3):617–e1
17. Long X, Liao W, Jiang C, Liang D, Qiu B, Zhang L (2012) Healthy aging: an automatic analysis of global and regional morphological alterations of human brain. Acad Radiol 19(7):785–793
18. Pienaar R, Fischl B, Caviness V, Makris N, Grant PE (2008) A methodology for analyzing curvature in the developing brain from preterm to adult. Int J Imaging Syst Technol 18(1):42–68
19. Poldrack RA (2007) Region of interest analysis for fMRI. Soc Cogn Affect Neurosci 2(1):67–70
20. Resnick SM, Pham DL, Kraut MA, Zonderman AB, Davatzikos C (2003) Longitudinal magnetic resonance imaging studies of older adults: a shrinking brain. J Neurosci 23(8):3295–3301
21. Rimol LM, Nesvag R, Hagler DJ, Bergmann O, Fennema-Notestine C, Hartberg CB, Haukvik UK, Lange E, Pung CJ, Server A, Melle I, Andreassen OA, Agartz I, Dale AM (2012) Cortical volume, surface area, and thickness in schizophrenia and bipolar disorder. Biol Psychiatry 71(6):552–560
22. Ronan L, Pienaar R, Williams G, Bullmore E, Crow TJ, Roberts N, Jones PB, Suckling J, Fletcher PC (2011) Intrinsic curvature: a marker of millimeter-scale tangential cortico-cortical connectivity? Int J Neural Syst 21(05):351–366
23. Segonne F, Dale AM, Busa E, Glessner M, Salat D, Hahn HK, Fischl B (2004) A hybrid approach to the skull stripping problem in MRI. Neuroimage 22(3):1060–1075
24. Segonne F, Pacheco J, Fischl B (2007) Geometrically accurate topology-correction of cortical surfaces using nonseparating loops. IEEE Trans Med Imaging 26(4):518–529
25. Shaw P, Kabani NJ, Lerch JP, Eckstrand K, Lenroot R, Gogtay N, Greenstein D, Clasen L, Evans A, Rapoport JL, Giedd JN, Wise SP (2008) Neuro developmental trajectories of the human cerebral cortex. J Neurosci 28(14):3586–3594
26. Silk TJ, Wood AG (2011) Lessons about neurodevelopment from anatomical magnetic resonance imaging. J Dev Behav Pediatr 32(2):158–168
27. Sonnenburg S, Ratsch G, Schafer C, Scholkopf B (2006) Large scale multiple kernel learning. J Mach Learn Res 7:1531–1565
28. Su L, Wang L, Chen F, Shen H, Li B, Hu D (2012) Sparse representation of brain aging: extracting covariance patterns from structural MRI. PLoS ONE 7(5):e36147
29. Taki Y, Thyreau B, Kinomura S, Sato K, Goto R, Kawashima R, Fukuda H (2011) Correlations among brain gray matter volumes, age, gender, and hemisphere in healthy individuals. PLoS ONE 6(7):e22734
30. Terribilli D, Schaufelberger MS, Duran FL, Zanetti MV, Curiati PK, Menezes PR, Scazufca M, Amaro E Jr, Leite CC, Busatto GF

(2011) Age-related gray matter volume changes in the brain during non-elderly adulthood. Neurobiol Aging 32(2):354–368
31. Tipping ME (2001) Sparse Bayesian learning and the relevance vector machine. J Mach Learn Res 1(3):211–244
32. Wang J, Dai D, Li M, Hua J, He H (2012) Human age estimation with surface-based features from MRI images. In: Wang F et al (eds) Machine learning in medical imaging. Springer, Berlin Heidelberg, pp 111–118
33. Wang Y, Fan Y, Bhatt P, Davatzikos C (2010) High-dimensional pattern regression using machine learning: from medical images to continuous clinical variables. Neuroimage 50(4):1519–1535
34. Youden WJ (1950) Index for rating diagnostic tests. Cancer 3(1):32–35